DISTURBANCE REJECTION DIFFERENTIAL TRACKING VARIABLE STRUCTURE CONTROLLER

Zhihuan Zhang* and Chao Hu**,***

Abstract

In view of the shortcomings of the traditional proportional, integral, and derivative controller, the active disturbance rejection control method is put forward, which extracts the differential and arranges the transition process reasonably through the "tracking differentiator" (TD) and the nonlinear state error feedback (NLSEF) controller. However, the current design of the NLSEF controller is only based on the experience to select the appropriate nonlinear function as there is no general theoretical guidance, so here we propose the active disturbance rejection sliding mode variable structure control method with extended state observer, in which a TD is used to process the reference input, a state observer to estimate the system state and the total disturbance, and the state error to formulate the switching function. This nonlinear variable structure control method realizes the excellent control for the robot joint and enhances the system anti-disturbance ability as well as the tracking accuracy.

Key Words

Arrangement of transition process, tracking differentiator, active disturbance rejection variable structure controller, robot joints

1. Introduction

The velocity closed-loop control is very important in precision servo robot system. High-performance velocity closed loop not only eliminates the system disturbances but also provides good object characteristics for a position loop [1]. Most of these control systems at present uses the classical proportional, integral, and derivative (PID) controller, because its structure is relatively simple and easy to be understood and does not depend on the object model. However, in the systems with strong interference or uncertainty, the PID controller often fails to achieve satisfactory results, so it is required to develop a control technique

* Ningbotech University, Ningbo, Zhejiang 315100, China, e-mail: zzh6488@163.com
** Jiaxing Research Institute, Southern University of Science and Technology, Jiaxing, Zhejiang 314000, China
*** $r\pi$ Tech (Shenzhen) Ltd., Shenzhen, Guangdong 518000, China; e-mail: huchao@nit.net.cn
Corresponding author: Chao Hu

with better performance than the PID controller [2]. The active disturbance rejection control (ADRC) method was proposed by Han Jingqing. It uses a tracking differentiator (TD) to process reference input and nonlinear state error feedback (NLSEF) to achieve a better performance of the controlled object. The extended state observer (ESO) is used to estimate the system state and total disturbance, which is independent of the object model and has good anti-interference ability. This method has been applied in the servo system successfully [3].

The ESO is a disturbance estimation technique [4], which expands the total disturbances (including the uncertain part of the model and the external disturbance) into the state quantity of the system and can estimate the total disturbances of the system when little model information is known. Due to its advantages of practicality and robustness, this control method based on ESO has been widely applied in the motor control [5], the missile guidance [6], the power conversion [7], and other areas.

The NLSEF controller is generally used empirically. According to the given signal obtained by the TD, the differential of the given signal and the error of the system output, as well as the derivative of the output observed by the state observer, the control, and disturbance compensation are carried out.

However, the conventional nonlinear ADRC is difficult to be further popularized in practical applications due to its complex design, numerous parameters, and difficult setting [8]. To solve these problems, Gao Zhiqiang proposed a linear state observer, which greatly reduced the number of setting parameters and achieved better performances.

It is well known that the PID control is based on the error to generate control strategy: eliminating the errors with the past, present, and variation trend of the weighted sum. Its advantages are [9]–[13]: depending on the error between the control goal and the actual behaviour to determine and eliminate the error of the control object, rather than relying on "input-output" relationship of the controlled object, that is, not on the input and output model of controlled object to determine the control strategy. It is simple and practicable to have the object to meet the static index as long as choosing the PID gain to make the closed loop stable. PID controller has disadvantages

as follows [14]–[17]: (a) when conventional PID system is used for correcting the closed-loop dynamic performance, it is too sensitive to the change of PID gain. When the controlled object is in a changing environment, PID gain is often required to be changed according to the change of environment. (b) "Eliminating error based on error feedback" is the essence of the PID control, but in the actual cases, directly taking the error between the target and the actual behaviour often might make the initial control too big to force the system response overshoot. That is what led to the main cause of irreconcilable contradiction between "quickness" and "overshoot" for the PID control closed-loop system. (c) PID uses the proportional, integral, and differential weights to maintain the feedback control quantity. In many cases, however, PI control law is adopted as there is no suitable differentiator, and it limits the performances of the PID control. (d) PID integral of the error feedback is effective to control constant disturbance, but in the absence of disturbance error, the integral feedback often makes worse the closed-loop dynamic characteristics. While for the disturbance changes at time, the inhibitory effect of integral feedback is not very significant. (e) PID is used to obtain the control quantity with the appropriate combination of past, present, and future errors. The classical PID generally adopts linear sum method, but the actual system is mostly nonlinear system, so nonlinear controller is more suitable.

On the deep understanding of traditional PID control technique, Han Jingqing *et al.* proposed an ADRC technique to avoid the shortcomings and to inherit the advantages of the PID control [18]. In view of the disadvantages of traditional PID, the ADRC was put forward, in which the "TD" is used to extract the differential quantity reasonably, the transition process is arranged appropriately, and the NLSEF controller is adopted properly. However, the NLSEF controller design is based on experience to choose the appropriate nonlinear function. There is no general theoretical instruction, so here we propose an immunity variable structure control method, where a TD is used as the reference input, an ESO to estimate the system state and total disturbance, and the state error to design the switch function. The nonlinear variable structure control method can realize the excellent control of the controlled object and enhance the disturbance rejection ability of the system as well as the tracking accuracy.

2. Arrange the Transition Process

Due to the limitation of cognitive level and technical conditions, if the PID controller extracts the error unreasonably, the direct determination of the reference input, the dynamic indicators (such as overshoot and transition process time), and the error of the system (as in most of the current control systems) will lead to a large overshoot. Therefore, here the idea of the arrangement of the transition process is put forward, in which the input increases slowly, making its difference with the output small, so as to reduce the overshoot as small as possible, and the steady state is reached, as shown in Fig. 1. The idea of "the arrangement of the transition process" is mainly to arrange dynamic
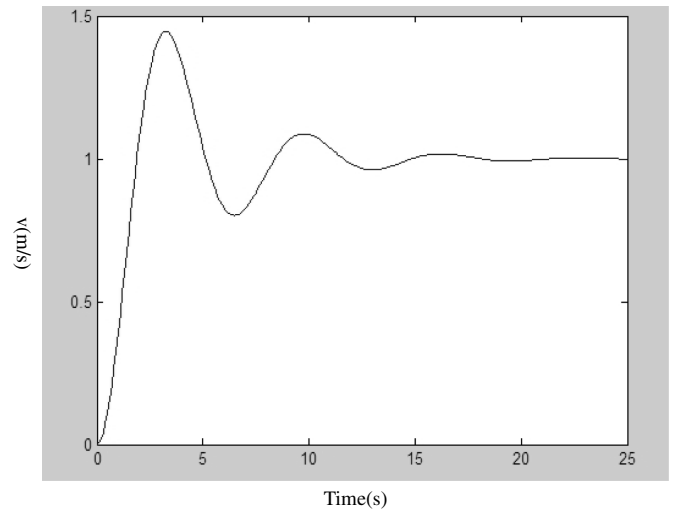
(a) Traditional PID control
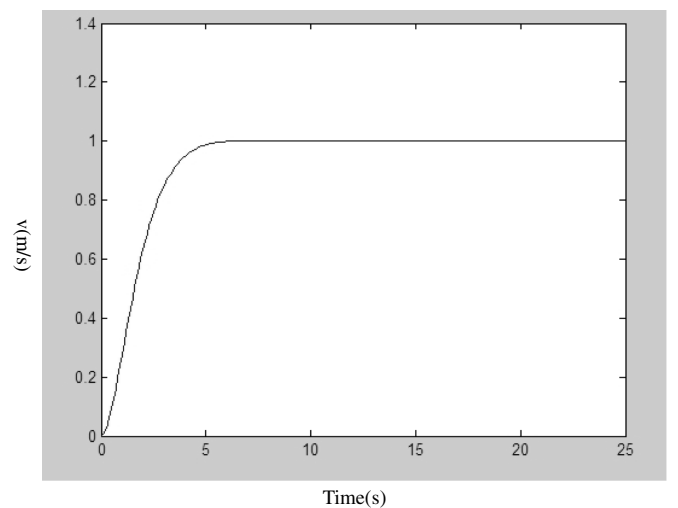
(b) Organizing the transition process

Figure 1. Comparison of overshoot and rapidity between traditional PID control and transition process arrangement.

process indicators to achieve optimal outputs, that is, the overshoot, and the adjustment time, instead of the static indicator: the reference input.

It can be seen that the contradiction between overshoot and rapidity can be solved by arranging the process. Moreover, the prior arrangement of transition process can enlarge the selection range of the error feedback gain and the error differential feedback gain, thus making their tuning easier [19]. In addition, the pre-set transition process can enlarge the range of object parameters that the given feedback gain can adapt to, that is, the controller is more robust.

3. Extracts Differentiation Reasonably by Tracking Differentiator

The traditional differential PID controller element to extract the differential error is unreasonable because the traditional differentiator is easy to cause severe noise amplifi-
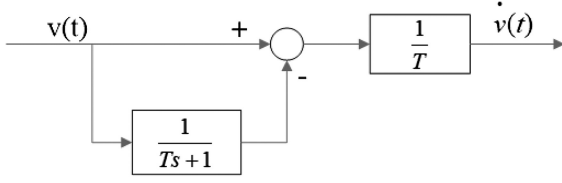
Figure 2. Equivalent block diagram of the classical differentiator.

Figure 3. General form of tracking differentiator.

cation effect if the input signal contains noise. Therefore, the TD [20], [21] is put forward to solve the problem of the noise amplification and the differential signal delay in the error signal. In the classical control theory, the differential of a given signal is obtained by the following transfer function of the differential element:

$$y = w(s)v = \frac{s}{Ts+1}v = \frac{1}{T}\left(1 - \frac{1}{Ts+1}\right)$$
$$v = \frac{1}{T}\left(v - \frac{1}{Ts+1}v\right) \tag{1}$$

where $w(s)$ is the classical differentiator; v is the input signal; and T is a relatively small differential time constant. It can be seen that the second term in the parentheses on the right of the above formula is the inertia link with time constant T, while the first term directly outputs the input signal, and its equivalent block diagram is shown in Fig. 2.

If the output of the second inertia link is recorded as $\bar{\nu}$, (1) satisfies the following equation:

$$y(t) = \frac{1}{T}(v(t) - \overline{v}(t)) \tag{2}$$

When the input signal $v(t)$ changes slowly and the time constant T is small, it can be regarded as a delay element, which can be obtained as:

$$\overline{v}(t) \gg v(t - T) \tag{3}$$

Therefore, (1) can be transformed into:

$$y(t) = \frac{1}{T}(v(t) - \bar{v}(t)) \approx \frac{1}{T}(v(t) - v(t-T)) \approx \dot{v}(t) \tag{4}$$

This is a differential element, where the smaller the time constant T, the closer the real differential. If the input signal is very pure and noise free, a better effect will be obtained. When the input signal $v(t)$ is polluted by some random noise $n(t)$, it can be obtained from (1) and (2):

$$y(t) = \frac{1}{T}(v(t) + n(t) - \overline{v(t) + n(t)}) \tag{5}$$

If the signal $v(t) + n(t)$ passes through the inertia element $\frac{1}{Ts+1}$ and gets the signal $\overline{y(t)} = \overline{v(t) + n(t)}$, it satisfies the differential equation:

$$\frac{d\bar{y}}{dt} = -\frac{1}{T}(\bar{y} - (v(t) + n(t))) \tag{6}$$

The solution of this equation is

$$\overline{y(t)} = \int_0^\infty e^{\frac{1}{T}(t-\zeta)}(v(\zeta) + n(\zeta))d\zeta$$
$$= \int_0^\infty e^{\frac{1}{T}(t-\zeta)}v(\zeta)d\zeta + \int_0^\infty e^{\frac{1}{T}(t-\zeta)}n(\zeta)d\zeta \tag{7}$$

Here, because $n(\zeta)$ is a high-frequency noise with a mean value of zero, the integral term $\int_0^\infty e^{\frac{1}{T}(t-\varsigma)}n(\varsigma)d\varsigma$ is almost equal to zero, and $\int_0^\infty e^{\frac{1}{T}(t-\varsigma)}v(\varsigma)d\varsigma \approx v(t-T)$, and the formula (5) can be modified into:

$$y(t) \approx \frac{1}{T}(v(t) + n(t) - v(t-T)) = \dot{v}(t) + \frac{1}{T}n(t) \tag{8}$$

That is, the output signal $y(t)$ is the differential signal of the input signal $v(t)$, superimposed with the amplified $\frac{1}{T}$ noise signal, so the smaller the T is, the more serious the noise amplification is, which is the principle of "noise amplification" effect of classical differentiator.

To eliminate or weaken the "noise amplification" effect, the differential approximation formula (4) is replaced by the following form:

$$\dot{v}(t) = \frac{v(t-\tau_1) - v(t-\tau_2)}{\tau_2 - \tau_1}, \quad 0 < \tau_1 < \tau_2 \tag{9}$$

The delay elements $v(t - \tau_1)$ and $v(t - \tau_2)$ are obtained respectively by the inertia elements $\frac{1}{\tau_1 s+1}$ and $\frac{1}{\tau_2 s+1}$ to reduce the "noise amplification" effect. The block diagram of its equivalent transfer function is shown in Fig. 3.

Then we can get

$$y = \frac{1}{\tau_2 - \tau_1}\left(\frac{1}{\tau_1 s+1} - \frac{1}{\tau_2 s+1}\right)$$
$$v = \frac{s}{\tau_1\tau_2 s^2 + (\tau_1 + \tau_2)s + 1}v \tag{10}$$

It can be seen that the "noise amplification" effect and the steady-state error can be reduced by introducing the TD. If the time constants τ_1 and τ_2 in (10) are very close to the constant τ, and let $\tau = \frac{1}{r}$, then the equation can be simplified to

$$w(s) = \frac{r^2 s}{s^2 + 2rs + r^2} \tag{11}$$

We can see that the differential function in (10) is to use the inertial element to track the dynamic characteristics of the input value as soon as possible (taking the small time constant) and to obtain the approximate differential signal by solving the differential equation. It is advisable

to divide $w(s)$ into two elements according to its function: $w_1(s) = \frac{r^2}{s^2+2rs+r^2}$ and $w_2(s) = s$. The step response of $w(s)$ can ensure that the setting value can be reached without overshoot and can be changed with the parameter r. Moreover, the bigger the r, the faster it reaches the set value. So, the TD has the function of arranging the transition process, which can be achieved only by adjusting r value. Obviously, the $w_2(s)$ produces the differential while $w_1(s)$ is used to track the reproduced signal, and the combination of the two elements can quickly obtain the differential. Therefore, the TD can be written in the following form:

$$\text{TD}: \begin{cases} \dot{v}_1 = v_2 \\ \dot{v}_2 = k^2(v - v_1) - 2k \cdot v_2 \end{cases} \tag{12}$$

where v is the input signal; v_1 is the output of $w_1(s)$, while v_2 is the obtained differential; k is the adjustment parameter, and the larger its value is, the faster the response is.

4. Basic Structure of Second-Order Active Disturbance Rejection Control

The ADRC system does not depend on the mathematical model and can maintain good dynamic and steady-state performances under the noises, the load disturbances, the mathematical model deviation, and the process parameter changes [22]. Its components include the TD, the ESO, the nonlinear anti-interference element (NLSEF), etc. In practice, the second-order ADRC is often used, as shown in Fig. 4, where the y and the v_0 are the output and the given input; the u is the control; and the w is the interference signal.

ESO can also be called the extended state observer with disturbance effect, which is the core of ADRC. The "model" of the controlled object and the "external disturbance" of the system are in the same position. The TD is used to arrange the appropriate "transition process" to solve the contradiction between "rapidity" and "overshoot" in PID control and improve the "robustness" of the system, where the nonlinear feedback is used to replace the calculation method of linear weighted summation in PID, so as to improve the performance of the controller [23].
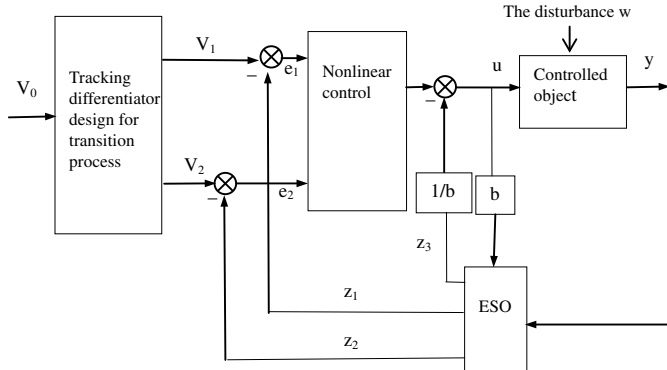
Figure 4. Basic structure of second-order ADRC.

Considering the unmodelled characteristics of the system and the effect of external disturbances, the second-order controlled object is approximately defined as

$$\ddot{y}(t) = f(t, y, \dot{y}, w) + bu \tag{13}$$

The second-order linear forms of ESO in ADRC are

$$\dot{z}_1 = z_2 + \beta_1(y - z_1) \tag{14}$$
$$\dot{z}_2 = z_3 + \beta_2(y - z_1) + Bu \tag{15}$$
$$\dot{z}_3 = \beta_3(y - z_1) \tag{16}$$

where β_1, β_2, β_3 are adjustable parameters; f represents the total error of the system; y, $\dot{y}$, $\ddot{y}$ are the observed estimates of the state, the differential signal, and the second-order differential of the object, respectively; z_1, z_2, z_3 are the observed estimates of y, $\dot{y}$, f; w is the unknown disturbance of the system, and b is the controller coefficient.

The second-order linear ADRC control law is expressed as:

$$u_0 = k_1(v_0 - z_1) - k_2 z_2 \tag{17}$$
$$u = (u_0 - z_3)/b \tag{18}$$

When ESO is implemented, the expected closed-loop transfer function can be obtained

$$\frac{y(s)}{v_0(s)} = \frac{k_1}{s^2 + k_2 s + k_1} \tag{19}$$

Aiming at the problem of multi-parameter debugging of the linear ADRC, the literatures [24], [25] list six parameters: b, k_1, k_2, β_1, β_2, β_3, that are required to be adjusted by the above formula, which can be reduced to four parameters: b, k_1, k_2, w_0.

5. Disturbance Rejection Differential Tracking Variable Structure Controller

PID controller only makes a simple weighted sum of the proportional, integral, and differential of the error, and its control efficiency is low. The efficiency of feedback control can be significantly improved by using the disturbance rejection differential tracking variable structure controller. Figure 5 shows a nonlinear disturbance rejection differential tracking variable structure controller composed of the TD, the ESO, and the variable structure controller. It can reasonably arrange the transition process, overcome the interferences, and achieve the perfect comprehensive results of the overshoot and the rapidity.

The proposed control algorithm is as follows:

Define $e_1(t) = v_1 - z_1$ and $e_2(t) = v_2 - z_2$, then we can get the correlation expression of the ESO:

$$e_{ESO}(t) = z_1 - y \tag{20}$$
$$\dot{z}_1 = z_2 - \beta_1 e_{ESO} \tag{21}$$
$$\dot{z}_2 = z_3 - \beta_2 e_{ESO} + b_0 u \tag{22}$$
$$\dot{z}_3 = -\beta_3 e_{ESO}(t) \tag{23}$$

where b_0 is the compensation factor. In ESO, it must be ensured that $\beta_1 > 0$, $\beta_2 > 0$, $\beta_3 > 0$, and $\beta_1 \beta_2 > \beta_3$. Moreover, the larger the β_1, the faster the tracking signal
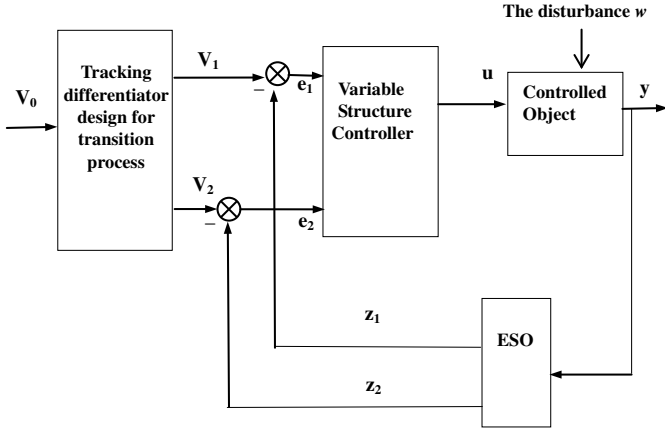
Figure 5. Variable structure control block diagram using tracking differentiator.

of the ESO; the larger the β_2, the faster the differential speed of the tracking signal of the ESO; and β_3 mainly affects the accuracy of the system. The smaller the β_3, the higher the system accuracy, but the estimation lag of the disturbances will increase, which may cause system oscillation and reduce the accuracy. Therefore, these three parameters of ESO should be configured reasonably.

Variable structure control design is as follows:

First, design the switching function:

$$s = c_1 e_1 + c_2 e_2 = c_1(v_1 - z_1) + c_2(v_2 - z_2) \qquad (24)$$

Then, we have

$$\dot{s} = c_1(\dot{v}_1 - \dot{z}_1) + c_2(\dot{v}_2 - \dot{z}_2) \qquad (25)$$

and

$$\begin{aligned} \dot{s} &= c_1(\dot{v}_1 - \dot{z}_1) + c_2(\dot{v}_2 - \dot{z}_2) \\ &= c_1(v_2 - z_2 + \beta_1 e_{ESO}) + c_2 \\ &\quad \times [k^2(v - v_1) - 2c_2 k \cdot v_2 - z_3 + \beta_2 e_{ESO} - b_0 u] \end{aligned} \qquad (26)$$

Switch the approach rate according to the index:

$$\dot{s} = -\varepsilon \operatorname{sgn}(s) - \lambda s \qquad \varepsilon \succ 0, \quad \lambda \succ 0, \qquad (27)$$

Then, the sliding mode variable structure control with ESO of the disturbance rejection TD is

$$\begin{aligned} u(t) &= \frac{1}{c_2 b_0}[\varepsilon \operatorname{sgn}(s) + \lambda s + c_1(v_2 - z_2 + \beta_1 e_{ESO}) \\ &\quad + c_2(k^2(v - v_1) - 2c_2 k \cdot v_2 - z_3 + \beta_2 e_{ESO})] \end{aligned} \qquad (28)$$

The optimal controller can be obtained by properly selecting the coefficients c_1, c_2.

6. Algorithm Simulation Results

The general robot joints are shown in Fig. 6 and the PD controller is usually used [24]–[27].

As the robot is generally a nonlinear system and its modelling is inaccurate, the control law for all joints in Fig. 6 could be:

$$\tau = K_p(q_d - q) - K_v \dot{q} \qquad (29)$$
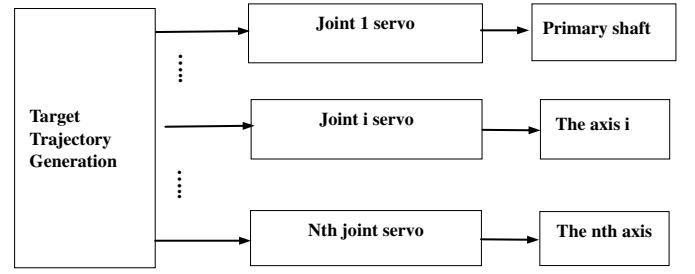
Figure 6. Robot servo system.

The proportional gain is $K_p = \operatorname{diag}(k_{pi})$, and the velocity feedback gain is $K_v = \operatorname{diag}(k_{vi})$. This joint servo system treats each joint as a simple single input and single output system, so its structure is simple.

However, there is a coupling effect among the joints, and each joint has to bear the disturbances caused by the motion of the other joints. In addition, the dynamics is nonlinear, and the parameters change with the motion of the joints [29], [30].

$$\tau = M(q)\ddot{q} + h(q, \dot{q}) + b\dot{q} + G(q) \qquad (30)$$

where the inertia matrix is $M(q) \in R^{n \times m}$; the vector of centrifugal force and Coriolis force is $h(q, \dot{q}) \in R^n$; $b \in R^{m \times n}$ represents the viscous friction coefficient matrix; the $G(q) \in R^n$ represents the vector of gravity term; and the joint drive vector is $\tau = [\, \tau_1 \ \tau_2 \ \cdot \ \tau_n \,]^T$.

Then the control rule is

$$\tau = K_p(q_d - q) - K_v \dot{q}_v \qquad (31)$$

These couplings are treated as external interferences. To compensate the influence of gravity term, we use

$$\tau = K_p(q_d - q) - K_v \dot{q}_v + G(q) \qquad (32)$$

But the control effect is not very good. In view of the above situation, an anti-disturbance differential tracking variable structure controller is applied and the robot joint is simulated. Taking the robot joint as the controlled object, the robot module includes a position loop and a velocity loop, which is equivalent to a second-order system, and the transfer function is expressed as:

$$G(s) = 133/s(s + 25) \qquad (33)$$

The command reference takes the sinusoidal signal $r(t) = 0.5\sin(6\pi t)$, in which the frequency is $f = 3$Hz; the controller parameters are reasonably selected and the initial interference takes -0.5. The simulation control results are shown in Fig. 7. It can be seen that the output y-out (the joint angle q radian) basically keeps up with the input r after 0.5 s. The switching function s (cm) is shown in Fig. 8, which finally reaches to 0 from the initial value 3. The controller output (N/cm) is shown in Fig. 9, and it can be seen that the controller output jitters in the sliding mode state.
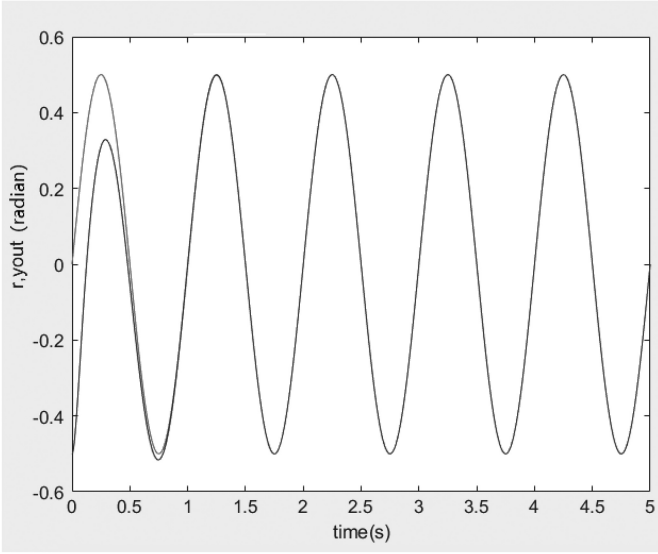
Figure 7. Sinusoidal tracking result.
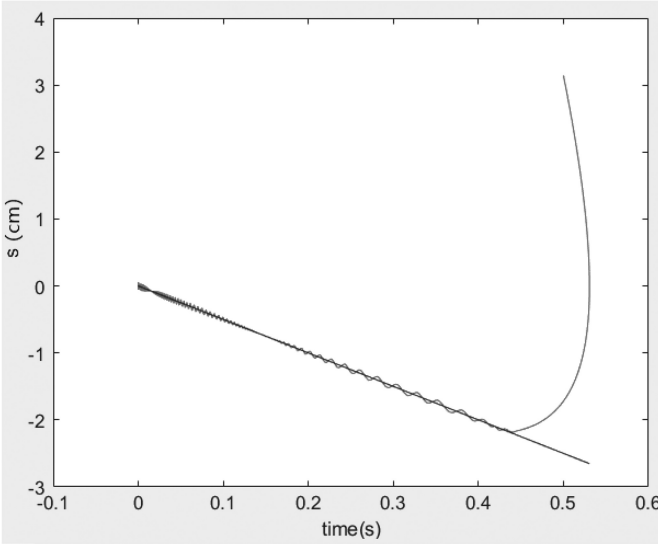
Figure 8. Switching function.
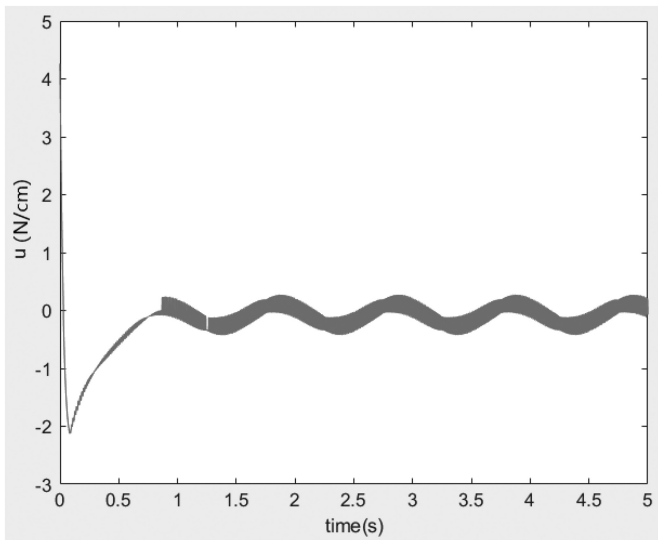
Figure 9. Controller output.

7. Conclusion

The core idea of ADRC is a kind of the effective data-driven mechanism, which estimates unknown unmodelled uncertainties and disturbances through the ESO. In the design of ADRC, the NLSEF controller only selects the appropriate nonlinear function according to the experience without general theoretical guidance. Therefore, we propose the ADRC variable structure control method, where the TD is used to process the reference input and the ESO of the system state and total disturbance are estimated. Then the state error is used to design the switching function, so the nonlinear variable structure control method is realized to obtain the satisfactory control of the controlled object, which can systematically reduce the influence of unmodelled uncertainty and disturbance.

As ADRC is essentially a model guided data-driven method, the application potential of ADRC in industry has been gradually found and has been successfully applied in the manufacturing process, the process control, the robot system, the energy system, and other fields. ADRC has been recognized as an effective alternative to PID control method. Therefore, the research on data-driven control and its application based on ESO and ADRC variable structure is of the fundamental significance for the development in various control fields.

Appendix

MATLAB Code:
```
clear all;
close all; global a b c A F M ep k
ts=0.001;
T=5;
TimeSet=[0:ts:T];

c=5.0;
para=[];

[t,x]=ode45('DynamicModel',TimeSet,[-0.5,0],[],para);
x1=x(:,1);
x2=x(:,2);

r=A*sin(2*pi*F*t);
dr=A*F*2*pi*cos(F*2*pi*t);
ddr=-A*(2*pi*F)^2*sin(2*pi*F*t);

s=c*(r-x(:,1)+dr-x(:,2));

if M==1
    slaw=-ep*sign(s)-k*s;
    u=1/b*(c*(dr-x(2))+ddr-slaw+a*x(2));
end

figure(1);
plot(t,r,'r',t,x(:,1),'b');
xlabel('time(s)');ylabel('r,yout');
figure(2);
plot(t,r-x(:,1),'r');
xlabel('time(s)');ylabel('error');
```

6

```
figure(3);
plot(r-x(:,1),dr-x(:,2),'r',r-x(:,1),-c*(r-x(:,1)),'b');
xlabel('time(s)');ylabel('s');
figure(5);
plot(t,u,'r');
xlabel('time(s)');ylabel('u');


function dx = DynamicModel(t,x,flag,para)
global a b c A F M ep k

a=25;b=133;

A=0.50;F=1.0;
r=A*sin(2*pi*F*t);
dr=A*F*2*pi*cos(F*2*pi*t);
ddr=-A*(2*pi*F)^2*sin(2*pi*F*t);

s=c*(r-x(1))+dr-x(2);

k=30;
ep=15;

M=1;
if M==1
  slaw=-ep*sign(s)-k*s;
end

  u=1/b*(c*(dr-x(2))+ddr-slaw+a*x(2));
  dx=zeros(2,1);
  dx(1)=x(2);
  dx(2)=-a*x(2)+b*u;
```

References

[1] L. Jinying, F. Chengyu, T. Tao, *et al.*, Design of self-reactive controller for photoelectric tracking system on motion platform, *Control Theory and Application*, *29*(7), 2012, 955–959.

[2] H. Jingqing, From PID technology to active disturbance rejection control technology, *Control Engineering*, *9*(3), 2002, 13–18.

[3] W. Shuai, L. Hongwen, M. Haoran, *et al.*, ADRC of velocity loop of photoelectric telescope servo system, *Optical Precision Engineering*, *19*(10), 2011, 2442–2449.

[4] J.Q. Han, From PID to active disturbance rejection control, *IEEE Transactions on Industrial Electronics*, *56*(3), 2009, 900–906.

[5] J.Y. Yao, Z.X. Jiao, and D.W. Ma, Adaptive robust control of DC motors with extended state observer, *IEEE Transactions on Industrial Electronics*, *61*(7), 2014, 3630–3637.

[6] Z. Zhu, D. Xu, J.M. Liu, *et al.*, Missile guidance law based on extended state observer, *IEEE Transactions on Industrial Electronics*, *60*(12), 2013, 5882–5891.

[7] B.S. Sun and Z.Q. Gao, A DSP-based active disturbance rejection control design for a 1-kW H-bridge DC-DC power converter, *IEEE Transactions on Industrial Electronics*, *52*(5), 2005, 1271–1277.

[8] G. Zhiqiang, Scaling and bandwidth-parameterization based controller tuning, *Proceedings of the American Control Conference*, Denver, Colorado, June 4–6, 2003, 4989–4996.

[9] M.A. Lotufo, L. Colangelo, C. Perez-Montenegro, E. Canuto, and C. Novara, UAV quadrotor attitude control: An ADRC-EMC combined approach, *Control Engineering Practice*, *84*(3), 2019, 13–22.

[10] L.A. Castañeda, A. Luviano-Juárez, G. Ochoa-Ortega, and I. Chairez, Tracking control of uncertain time delay systems: An ADRC approach, *Control Engineering Practice*, *78*(9), 2018, 97–104.

[11] Y. Wu and Q. Zheng, ADRC or adaptive controller – A simulation study on artificial blood pump, *Computers in Biology and Medicine*, *66*(C), 2015, 135–143.

[12] Z.-H. Wu and B.-Z. Guo, Approximate decoupling and output tracking for MIMO nonlinear systems with mismatched uncertainties via ADRC approach, *Journal of the Franklin Institute*, *355*(9), 2018, 3873–3894.

[13] S. Luo, Q. Sun, M. Sun, P. Tan, W. Wu, H. Sun, and Z. Chen, On decoupling trajectory tracking control of unmanned powered parafoil using ADRC-based coupling analysis and dynamic feedforward compensation, *Nonlinear Dynamics*, *92*(4), 2018, 1619–1635.

[14] H. Chen, Y. Sun, T. Yang, and Y. Huang, Design of MMC-STATCOM controller based on ADRC technology, *Application of Electronic Technology*, *46*(2), 2020, 114–120.

[15] Z. Huang, C. Zhang, Y. Zhang, and G. Zhang, A data-driven online ADP control method for nonlinear system based on policy iteration and nonlinear MIMO decoupling ADRC, *Neurocomputing (Amsterdam)*, *310*(10), 2018, 28–37.

[16] Z. Yang, Z. Wang, and M. Yan, An optimization design of adaptive cruise control system based on MPC and ADRC, *Actuators*, *10*(6), 2021, 110–128.

[17] S. Yao, G. Gao, and Z. Gao, On multi-axis motion synchronization: The cascade control structure and integrated SMC-ADRC design, *ISA Transactions*, *109*(3), 2021, 259–268.

[18] C. Mohssine, N. Tamou, and E. Ahmed, Contribution of variable speed wind turbine generator based on DFIG using ADRC and RST controllers to frequency regulation, *International Journal of Renewable Energy Research*, *111*(1), 2021, 320–331.

[19] S. Chen; W. Xue, S. Zhong, and Y. Huang, On comparison of modified ADRCs for nonlinear uncertain systems with time delay, *Science China. Information Sciences*, *61*(7), 2018, 1–15.

[20] I. Minka, A. Essadki, and T. Nasser, The ADRC linear power control applied to the wind turbine system based on DFIG, *ARPN Journal of Engineering and Applied Sciences*, *13*(14), 2018, 4378–4386.

[21] F. Yang, C. Guo, and Y. Jiang, RBF based Integrated ADRC Controller for a Ship Dynamic positioning system, *Proceedings of 2017 Chinese Intelligent Automation Conference*, Lecture Notes in Electrical Engineering, 2018, 673–680.

[22] H.-b. Gan and B. Lv, Research on drum water level control of marine auxiliary boiler based on ADRC, *Polish Maritime Research*, *25*(2), 2018, 35–41.

[23] Z. Gao, Research on active disturbance rejection control, *Control Theory and Application*, *30*(12), 2013, 1498–1508.

[24] F. Basile, P. Chiacchio, and D. Del Grosso, Implementation of hydraulic servo controllers with only position measure, *International Journal of Robotics and Automation*, *24*(1), 2009, 20–37.

[25] R. Garrido and L. Luna, Robust ultra-precision motion control of linear ultrasonic motors: A combined ADRC-Luenberger observer approach, Control Engineering Practice, *111*(6), 2021, 104812–104823.

[26] M. Sun, Y. Gao, W. Liu, and S. Li, Data-efficient model-based reinforcement learning for robot control, *International Journal of Robotics and Automation*, *36*(4), 2021, 211–218.

[27] S. Zhong, Y. Huang, and L. Guo, An ADRC-based PID tuning rule, *International Journal of Robust and Nonlinear Control*, 2021, 1–14.

[28] S. Kaitwanidvilai, P. Olranthichachat, and I. Ngamroo, Weight optimization and structure-specified robust H$^\infty$ loop-shaping control of a pneumatic servo system using genetic algorithm, *International Journal of Robotics & Automation*, *25*(3), 2010, 229–239.

[29] W. Lu, Q. Li, K. Lu, Y. Lu, L. Guo, W. Yan, and F. Xu, Load adaptive PMSM drive system based on an improved ADRC for manipulator joint, *IEEE Access*, *9*(3), 2021, 33369–33384.

[30] Z. Hua, X. Rong, Y. Sun, Y. Li, H. Chai, & C. Wang, A novel passive compliance method for hydraulic servo actuator applied on quadruped robots, *International Journal of Robotics and Automation*, *37*(1), 2022, 76–87.

Biographies

Zhihuan Zhang received bachelor degree of electrical engineering and master degree of automation and computer engineering from Wuhan University of Technology, Wuhan, China, in 1988 in 1985; and Ph.D. degree of control science and engineering from the Zhejiang University, Hangzhou, China, in 2002. He started to work as a teacher in the Ningbo University. From 2004 to 2005, he visited at University of Alberta, Edmonton, Canada. Now he is an Associate Professor in NingboTech University, Ningbo, China.

His research focuses on the robot control, Artificial intelligence and information visualization, electrical engineering and control systems. He has authored or co-authored more than thirty research papers, applied more than twenty-eight patents, and chaired more than sixteen national and industrial research projects.

Chao Hu (Corresponding Author) received the B.S. degree in electrical engineering and the M.S. degree in optical engineering from Zhejiang University, Hangzhou, China, in1982 and 1986, and the Ph.D. degree in electrical and computer engineering from University of Alberta, Edmonton, Canada, in 2006. From 1986 to 2001, he was a staff member in Ningbo University, Ningbo, China. From 2006 to 2011, he was a Research Professor with the Shenzhen Institute of Advanced Technology, Chinese Academy of Sciences, Shenzhen, China. From 2011 to 2020, he was a Professor in Ningbo Tech University, Ningbo, China. Currently, he is a research member in Jiaxing Research Institute, Southern University of Science and Technology, Jiaxing, Zhejiang, China, and a deputy general manager in $r\pi$ Tech (Shenzhen) Ltd., Shenzhen, Guangdong, China.

He has authored more than 230 research papers, applied more than 30 patents, and chaired more than 30 national, local, and industrial research projects. His primary research interests include the areas of intelligent sensors, computer vision, medical electronics, and intelligent localization systems.